Available online at www.sciencedirect.com
ScienceDirect
Ceramics International 34 (2008) 1393–1397
CERAMICS INTERNATIONAL
www.elsevier.com/locate/ceramint

Growth behavior, morphology and properties of lithium aluminosilicate glass ceramics with different amount of CaO, MgO and TiO_2 additive

A.M. Hu *, M. Li, D.L. Mao

The State Key Laboratory of the Metal Matrix Composites, School of Materials Science and Engineering, Shanghai Jiaotong University, Shanghai 200030, PR China

Received 22 September 2006; received in revised form 2 January 2007; accepted 24 March 2007
Available online 17 May 2007

Abstract

Li_2O–Al_2O_3–SiO_2 glass with CaO, MgO and TiO_2 additive were investigated. With more CaO + MgO addition, the crystallization temperature (T_p) and the value of Avrami constant (n) decreased, the activation energy (E) increased. The mechanism of crystallization of the glass ceramics changed from bulk crystallization to surface crystallization. With more TiO_2 addition, the crystallization temperature decreased, E and n had a little change. The crystallization of the glass ceramics changed from surface crystallization to two-dimensional crystallization. Plate-like, high mechanical properties spodumene-diopside glass ceramics were obtained. The mechanical properties related with crystallization and morphology of glass ceramics.

Keywords: A. Grain growth; C. Mechanical properties; D. Glass; D. Glass ceramics; Crystallization

1. Introduction

Glass ceramics have been investigated for more than three decades. It is important to design the composition and control the crystallization of the glass to achieve desired microstructure and properties [1–3]. Lithium aluminosilicate (LAS) glass ceramics have gained considerable attention because of their very low thermal expansion coefficient (CTE), high transparency, excellent thermal shock resistance and chemical durability [1–4]. In LAS glass ceramics, the ultralow thermal expansion is due to the main crystalline phases: β-quartz solid solution (Li_2O–Al_2O_3–$2SiO_2$) and β-spodumene (Li_2O–Al_2O_3–$4SiO_2$), but there are some disadvantages: they have low strength (100 MPa for high-quartz and 140 MPa for β-spodumene), and the glass ceramics need high temperature (above 1873 K) to produce them. To lower the melting temperature, the fluxes such as alkali oxides, alkali earth oxides, lanthanon metal oxides, B_2O_3, P_2O_5 and F^- have been added in LAS glass ceramics for many years [5–15]. But these additions could not solve the problems of lower strength at the same time. Diopside glass ceramics ($CaO{\cdot}MgO{\cdot}2SiO_2$) has higher bending strength (300 MPa) and fracture toughness (3.5 MPa $m^{1/2}$) [16–20]. Ashizuka had reported that in CaO–MgO–SiO_2–P_2O_5 system with diopside and apatite as main phase, the glass ceramics had high strength (about 236 MPa) [17]. It is desired to produce a glass ceramics with two phases: spodumene and diopside, this glass ceramics will have low thermal expansion and high mechanical properties.

In the present work, different amount of CaO, MgO and TiO_2 were added to lithium aluminosilicate glass to obtain spodumene-diopside glass ceramics with high strength and low melting temperature. The growth behavior, morphology and properties of the spodumene-diopside glass ceramics were also investigated.

2. Experimental procedures

The starting materials were analytical grade: SiO_2, Al_2O_3, MgO, Li_2CO_3, $CaCO_3$, ZnO and TiO_2. The detailed compositions of the glasses are given in Table 1. Glass batches were melted in alumina crucibles at 1773–1873 K for 2 h according to the composition. Then the glass were anneal at 873 K for 1 h. Homogeneous, transparent glasses were obtained from all compositions.

* Corresponding author. Tel.: +86 21 62932522; fax: +86 21 62932522.
E-mail address: huanmin@tsinghua.org.cn (A.M. Hu).

0272-8842/$34.00
doi:10.1016/j.ceramint.2007.03.032

Table 1
Composition of the glasses (wt.%)

No.	Li_2O	Al_2O_3	SiO_2	ZnO	MgO	CaO	TiO_2
1	4.0	20.0	66.0	2.0	1.0	1.0	6.0
2	3.8	18.2	64.1	1.9	3.0	3.0	6.0
3 (T2)	3.6	17.0	60.6	1.8	5.5	5.5	6.0
4	3.4	15.6	56.3	1.7	8.5	8.5	6.0
T1	3.7	17.4	61.9	1.8	5.6	5.6	4.0
T3	3.5	16.5	58.7	1.7	5.3	5.3	9.0
T4	3.4	16	56.7	1.7	5.1	5.1	12.0

Differential thermal analysis (DTA) of annealed glass specimens were carried out in a Dupont 2100 Thermal Analyzer. The quenched glasses were ground and screened to about 200 μm. Non-isothermal experiments were performed by heating 30 mg samples in a Pt crucible with Al_2O_3 as the reference material in the temperature range between 293 and 1473 K at 5–20 K/min under a flowing atmosphere of drying air (30 cm^3/min).

X-ray diffraction (XRD) investigations were made using a D-max-RB diffractometer with Cu Kα radiation in the 2θ range from 10° to 70° at 0.02° steps.

Scanning electron microscopy (SEM) was conducted with a JSM-6301F. Specimens were prepared with standard metallographic techniques followed by chemical etching in an HF solution (5%) for 90 s. Etched glass ceramic samples were coated with a thin layer of gold.

The strength was measured in 10 specimens for each glass ceramics sample (4 mm × 3 mm × 36 mm) using four-point bending strength with a span of 30 mm at a crosshead speed of 0.5 mm per 60 s. The fracture toughness was measured by an indentation fracture (IF) method using the Evans equation to calculate K_{IC} from the length of the crack and the semi-diagonal of the indentation [21].

3. Results and discussion

3.1. DTA results

DTA curves for the four glass samples with particle sizes 200 μm obtained at a heating rate of 10 K/min are shown in Fig. 1. The CaO, MgO can serve as network modifiers to reduce the melting point and viscosity of the glass; it can be seen from Fig. 1(a) that with more CaO + MgO addition, the glass crystallization peak temperatures decrease, from 1139 to 1068 K, with more TiO_2 addition, the glass crystallization peak temperatures decrease, from 1103 to 1054 K.

The kinetics of crystal growth in glass can be described using the Johnson–Mehl–Avrami (JMA) equation [22–24]:

$$-\ln(1-x) = (kt)^n \tag{1}$$

where x is the volume fraction of crystallized phase at time t, n the Avrami exponent related to the mechanism of crystallization, and k is the reaction rate constant, related to the absolute temperature T, by Arrhenius type equation:

$$k = \nu \exp\left(-\frac{E}{RT}\right) \tag{2}$$

where ν is the frequency factor, R the gas constant and E is activation energy of crystal growth.

Starting from Eqs. (1) and (2), non-isothermal crystallization kinetics of glass can be described by the expression [22–24]:

$$\ln\frac{T_p^2}{\alpha} = \frac{E}{RT_p} + \ln\frac{E}{R\nu} \tag{3}$$

where T_p is the crystallization peak maximum temperature in a DTA curve, α the heating rate of DTA, R the gas constant and E is the activation energy of crystal growth. Values of E can be calculated by Eq. (3) by plots of $\ln(T_p^2/\alpha)$ versus $1/T_p$ which are shown in Fig. 2, and the results are given in Table 2. With more CaO and MgO addition, the activation energy of crystal growth E, corresponding to the energy barrier of transition from glass to crystal, increases from 299 to 537 kJ/mol, this means that the glass crystallization become more difficult with more CaO and MgO addition. With TiO_2 addition, E decreases from 524 to 485–494 kJ/mol.

The Avrami parameter n was calculated by the Augis–Bennett equation [25]:

$$n = \frac{2.5}{\Delta T} \times \frac{RT_p^2}{E} \tag{4}$$

where ΔT is the full width of the exothermic peak at the half maximum intensity. The Avrami parameter, $n = 1$ indicates one-dimensional growth (surface crystallization), $n = 2$ indicates two-dimensional crystallization, and $n = 3$ implies three-dimensional growth (bulk crystallization) [12–17]. The values of n calculated by Eq. (4) for four glasses are 3.2, 2.6, 1.9 and 1.4 (Table 2). This means that the crystallization mechanism

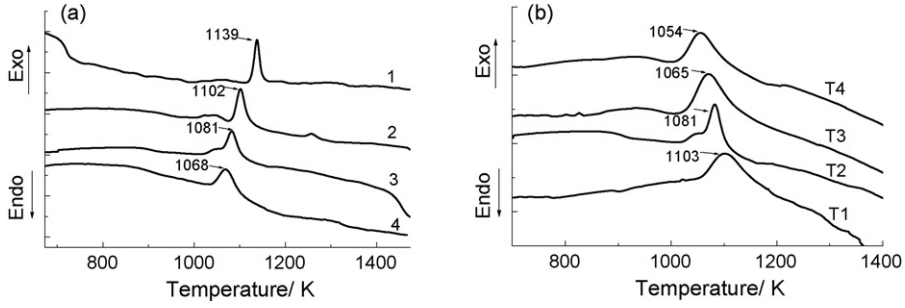

Fig. 1. DTA curves of glass samples, α = 10 K/min.

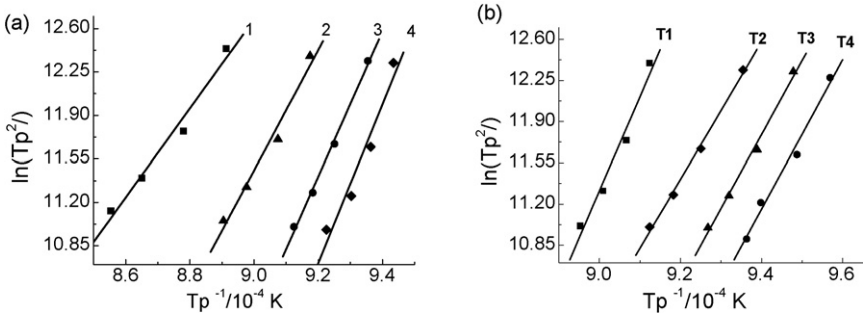

Fig. 2. Plots of $\ln(T_p^2/\alpha)$ vs. $1/T_p$ for the four glasses.

Table 2
The values of activation energy E and Avrami parameter n for crystal growth

	No.						
	1	2	3 (T2)	4	T1	T3	T4
E (kJ/mol)	299 ± 3	403 ± 4	485 ± 3	537 ± 5	524 ± 5	482 ± 3	498 ± 3
n	3.2 ± 0.3	2.6 ± 0.2	1.9 ± 0.3	1.4 ± 0.2	1.3 ± 0.2	2.0 ± 0.3	1.7 ± 0.2

changes from bulk to surface crystallization with more CaO + MgO addition. With TiO_2 addition increasing from 4% to 12%, n increases from 1.3 to only 1.8–2.0, this mean that TiO_2 can increase the crystallizations in this glass system, but it is not an optimum nucleating agent.

3.2. XRD results

Fig. 3 illustrates the powder XRD patterns of the glasses heat-treated at 1323 K for 2 h. Fig. 3(a) shown that in sample 1 and sample 2, the main phase was β-spodumene, no diopside appeared. CaO and MgO may enter into the h-quartz or β-spodumene structure. With more CaO + MgO addition, as in sample 3 and sample 4, the content of diopside increased at the expense of β-spodumene. A trace of h-quartz solid solution still appeared in all samples. Fig. 3(b) shown that with more TiO_2 addition, some TiO_2 appears besides the main phase β-spodumene and diopside.

3.3. Microstructures

Fig. 4 shows SEM micrographs of the glass ceramic samples with different amount of CaO + MgO and TiO_2 additive heat-treated at 1323 K for 2 h. Samples 1 and 2 showed homogeneous dispersion of tiny spherical crystallites, the grain sizes were 1–2 μm (Fig. 4(a) and (b)). This indicates that the crystallization mechanism is bulk crystallization. With more CaO + MgO addition, as in sample 3, there are plate-like crystals instead of tiny spherical crystals, and the grain sizes increase to about 3–4 μm. With even more CaO + MgO addition, as in sample 4, the crystallization is observed to start at surface of the glasses sample, and then proceeds towards the interior of the glass matrix, and coarse dendritic formations appear. These results are in agreement with the above analysis of crystallization kinetics. Namely, the crystallization mechanism changes from bulk crystallization to surface crystallization with CaO + MgO addition.

With 4%TiO_2 addition, the coarse dendritic grain appeared, the same as sample 4 (not shown here). As the TiO_2 content increased to 6%, plate-like crystals appeared; this means that the crystallization changed from bulk to surface crystallization, i.e. the crystallization mechanism changes from one-dimensional to two-dimensional with TiO_2 content increasing from 4% to 6%. On the contrary, with more TiO_2 (9% and 12%) addition (samples T3 and T4), the glass ceramics almost have the same morphology as sample T2 (6%TiO_2).

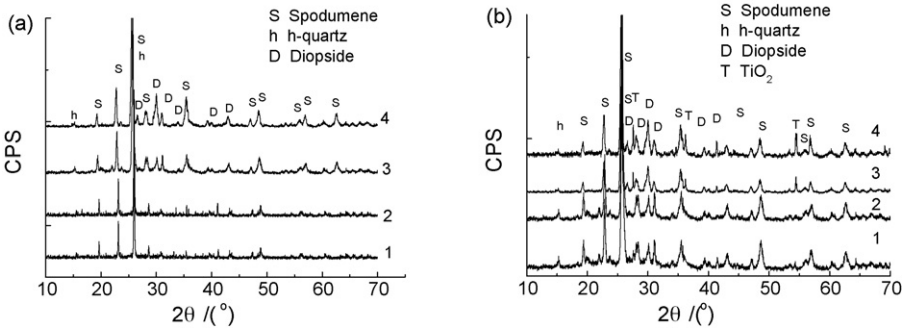

Fig. 3. XRD patterns of the glass ceramics samples heat-treated at 1323 K/2 h.

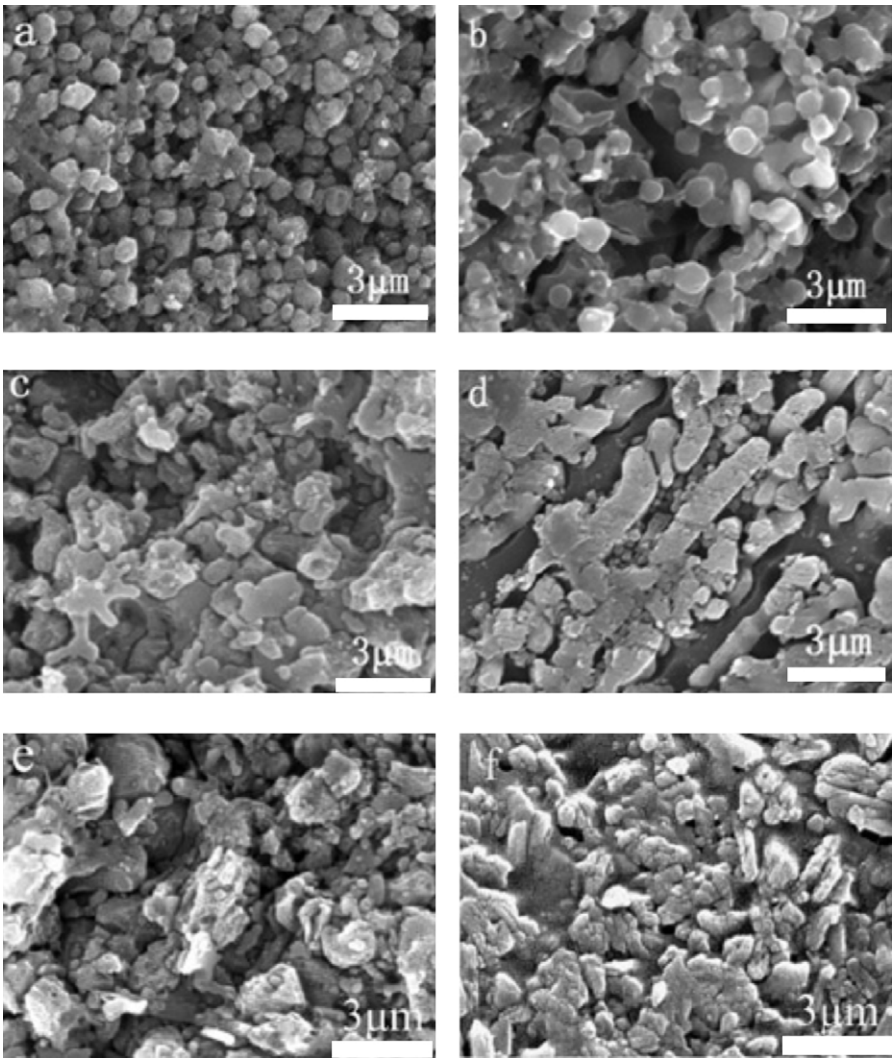

Fig. 4. SEM photographs of sample 1 (a), sample 2 (b), sample 3/T3 (c), sample 4 (d) and sample T3 (e), sample T4 (f) heat-treated at 1323 K/2 h.

3.4. Mechanical properties

The mechanical properties of the glass ceramics with different amount of CaO, MgO and TiO_2 addition after crystallization at 1323 K/2 h are given in Table 3. With more CaO + MgO addition, diopside increased at the expense of β-spodumene (CTE is 3–9 × 10^{-7} K^{-1}) [1–5], as diopside has a high positive thermal expansion coefficient (CTE is 50–150 × 10^{-7} K^{-1}) [15], the thermal expansion coefficients increases.

The values of Vickers hardness, elastic moduli, flexural strength and fracture toughness have different trends and the sample 3 has the maximum values. The properties of glass ceramics are correlated with crystallization and morphology. After crystallization at 1323 K/2 h, the main phase of sample 1 is β-spodumene, so the samples have almost the same properties as pure β-spodumene, which exhibits a flexural strength 140 MPa [1–3]. With more CaO + MgO addition, as in sample 3, a spodumene-diopside compound appears. Owing to

Table 3
The mechanical properties of spodumene-diopside glass ceramics heat-treated at 1323 K for 2 h

No.	The Vickers hardness (GPa)	Elastic moduli (GPa)	Flexural strength (MPa)	Fracture toughness (MPa $m^{1/2}$)	Thermal expansion coefficient (K)
1	6.3	91	138	1.6	7.4 × 10^{-7}
2	6.2	87	134	1.5	9.9 × 10^{-7}
3 (T2)	6.8	93	199	2.4	12.8 × 10^{-7}
4	6.4	89	152	1.9	19.3 × 10^{-7}
T1	6.3	86	138	1.9	
T3	6.8	91	193	2.1	14.7 × 10^{-7}
T4	6.6	89	172	1.9	18.9 × 10^{-7}

higher flexural strength (300 MPa) of diopside [16–18] and the plate-like interlock morphology, sample 3 has flexural strength values (199 MPa) higher than with pure β-spodumene and lower than with pure diopside (300 MPa) [16–20]. In sample 4, although more diopside precipitated, the coarse dendritic grain lowers the mechanical properties according to Hall–Petch relationship [26,27].

With more TiO_2 addition, the thermal expansion coefficient increased, the mechanical properties of the glass ceramics, such as the values of Vickers hardness, elastic moduli, flexural strength and fracture toughness, increased from 4% to 6%, then decreased from 6% to 9% and 12%. This means that extra TiO_2 addition is disadvantage to the glass ceramics.

4. Conclusions

Spodumene-diopside glasses ceramics were obtained with CaO + MgO addition. As the CaO + MgO content increased, the crystallization temperature decreased, and the crystallization of the glass ceramics changed from bulk crystallization to surface crystallization, the grain sizes and thermal expansion coefficients increased, while the flexural strength and fracture toughness of the glass ceramics reached a maximum value with 5.5%CaO + 5.5%MgO addition. The mechanical properties were correlated with crystallization and morphology of glass ceramics. The crystallization mechanism changes from one-dimensional to two-dimensional crystallization as TiO_2 content increases from 4% to 6%, while all higher amount of TiO_2 (9% and 12%) is disadvantageous to the glass ceramics.

Acknowledgements

This work was financially supported by Shanghai Nanotechnology Promotion Center (Contract No. 0352nm062) and China Postdoctoral Science Foundation.

References

[1] G.H. Beall, L.R. Pinckney, Nanophase glass-ceramics, J. Am. Ceram. Soc. 82 (1) (1999) 5–16.
[2] L. Arnault, M. Gerland, A. Riviere, Microstructural study of two LAS-type glass-ceramics and their parent glass, J. Mater. Sci. 35 (9) (2000) 2331–2345.
[3] P. Riello, P. Canto, N. Comelato, et al., Nucleation and crystallization behavior of glass-ceramic materials in the Li_2O–Al_2O_3–SiO_2 system of interest for their transparency properties, J. Non-Cryst. Solids 288 (2001) 127–133.
[4] M. Guedes, A.C. Ferro, J.M.F. Ferreira, Nucleation and crystal growth in commercial LAS compositions, J. Eur. Ceram. Soc. 21 (2001) 1187–1194.
[5] A.M. Hu, K.M. Liang, P. Fei, H. Shao, Crystallization and microstructure changes in fluorine-containing Li_2O–Al_2O_3–SiO_2 glasses, Thermochim. Acta 413 (1–2) (2004) 53–55.
[6] C. Leonelli, T. Manfredini, M. Paganelli, et al., Li_2O–Al_2O_3–SiO_2–$Me^{II}O$ glass-ceramic systems for tile glaze application, J. Am. Ceram. Soc. 74 (5) (1991) 983–987.
[7] M.C. Wang, M.H. Hon, F.S. Yen, Growth behavior and morphology of lithium–calcium aluminosilicate (LCAS) glasses, J. Cryst. Growth 91 (1988) 155–162.
[8] K.J. Anusavice, N.Z. Zhang, Effect of crystallinity on strength and fracture toughness of Li_2O–Al_2O_3–CaO–SiO_2 glass-ceramics, J. Am. Ceram. Soc. 80 (1997) 1353–1358.
[9] J.J. Shyu, M.T. Chiang, Sintering and phase transformation in B_2O_3/P_2O_5-doped $Li_2O{\cdot}Al_2O_3{\cdot}4SiO_2$ glass-ceramics, J. Am. Ceram. Soc. 83 (2000) 635–639.
[10] K. Davkova, S. Zafirovski, S. Pocev, V. Zlatanovic, Preparation of precipitated batch composition for glass ceramics in the system SiO_2–Al_2O_3–Li_2O–TiO_2–B_2O_3–ZnO–MgO, Glass Technol. 41 (2000) 197–198.
[11] J.J. Shyu, C.S. Hwang, Effects of Y_2O_3 and La_2O_3 addition on the crystallization of $Li_2O{\cdot}Al_2O_3{\cdot}4SiO_2$ glass-ceramic, J. Mater. Sci. 31 (1996) 2631–2639.
[12] A.M. Hu, K.M. Liang, F. Zhou, H. Shao, The nucleation and crystallization behavior of Li_2O–Al_2O_3–SiO_2 glasses with CeO_2 addition, Ceram. Int. 31 (2005) 11–14.
[13] L. Barbieri, A.B. Corradi, C. Leonelli, C. Siligardi, T. Manfredini, G.C. Pellacani, Effect of TiO_2 addition on the properties of complex aluminosilicate glasses and glass-ceramics, Mater. Res. Bull. 32 (6) (1997) 637–648.
[14] J. Rincon, M. Romero, M. Marco, et al., Some aspect of crystallization microstructure on new glass-ceramic glazes, Mater. Res. Bull. 33 (8) (1998) 1159–1164.
[15] A.W.A. Elshennawi, E.M.A. Hamzawy, G.A. Khater, A.A. Omar, Crystallization of some aluminosilicate glasses, Ceram. Int. 27 (2001) 725–730.
[16] M. Romero, J.Ma. Rincón, A. Acosta, Effect of iron oxide content on the crystallisation of a diopside glass–ceramic glaze, J. Eur. Ceram. Soc. 22 (2002) 883–890.
[17] M. Ashizuka, E. Ishida, Mechanical properties of silicate glass–ceramics containing tricalcium phosphate, J. Mater. Sci. 32 (1997) 185–188.
[18] P. Alizadeh, V.K. Marghussian, The effect of compositional changes on the crystallization behavior and mechanical properties of diopside wollostanite glass-ceramics in the SiO_2–CaO–MgO–(Na_2O) system, J. Eur. Ceram. Soc. 20 (2000) 765–773.
[19] R. Cio, P. Pernice, A. Aronne, G. Quattroni, Nucleation and crystal growth in fly ash derived glass, J. Mater. Sci. 28 (1993) 6591–6594.
[20] E.M. Kucukbayrak, S. Ersoymericboyu, M.L. Aovecoglu, Crystallization behaviour of glasses produced from fly ash, J. Eur. Ceram. Soc. 21 (2001) 2835–2841.
[21] Y.M. Sung, J.H. Sung, Calcia-alumina fibre reinforced beta -spodumene glass-ceramic matrix composites, J. Mater. Sci. Lett. 16 (1997) 1527–1529.
[22] M. Avrami, Kinetics of phase change, J. Chem. Phys. 7 (9) (1939) 1103–1112, 177–184.
[23] W.A. Johnson, K.F. Mehl, Reaction kinetics in process of nucleation and growth, Trans. AIME 135 (1939) 416–442.
[24] H.E. Kissinger, Variation of peak temperature with heating rate in differential thermal analysis, J. Res. Natl. Bureau Stand. 57 (1956) 217–221.
[25] J.A. Augis, J.E. Bennett, Calculation of the Avrami parameters for heterogeneous solid-state reactions using a modification of the Kissinger method, J. Therm. Anal. 13 (1978) 283–292.
[26] E.O. Hall, The deformation and aging of mild steel. III. Discussion of results, Proc. Phys. Soc. London B 64 (1951) 747–753.
[27] N.J. Petch, The cleavage strength of polycrystals, J. Iron Steel Inst. 174 (1953) 25–28.